ICASSP 2023 - 2023 IEEE International Conference on Acoustics, Speech and Signal Processing (ICASSP) | 978-1-7281-6327-7/23/$31.00 ©2023 IEEE | DOI: 10.1109/ICASSP49357.2023.10094780

ITER-SIS: ROBUST UNLIMITED SAMPLING VIA ITERATIVE SIGNAL SIEVING

Ruiming Guo and Ayush Bhandari

Dept. of Electrical and Electronic Engg., Imperial College London, SW7 2AZ, UK.
Email: `{ruiming.guo,a.bhandari}@imperial.ac.uk` or `ayush@alum.mit.edu`

ABSTRACT

Unlimited Sampling Framework (USF) is a digital acquisition protocol that recovers high dynamic range (HDR) input signals from their low dynamic range, modulo samples. Current USF theory and algorithms are predominantly focused on bandlimited signal classes that rely on a relatively high sampling rate. Recently, the "Fourier-Prony" algorithm was proposed and validated via hardware experiments with modulo ADCs. It was shown that this algorithm offers competitive performance in the presence of system noise and quantization, especially when periodic boundary conditions are satisfied.

In practice, signals are often measured over a finite observation window and this implies leakage in the Fourier domain. Depending on the severity of spectral leakage, Fourier domain algorithms may fail to reconstruct. To overcome this bottleneck, in this paper, we propose an **Iter**ative **Si**gnal **S**ieving Algorithm (ITER-SIS) that solely operates in the time domain. By utilizing a continuous-domain characterization of modulo samples, ITER-SIS achieves a robust, low-sampling-rate, FFT-free recovery of signals with a finite time observation window, even when there is considerable spectral leakage. Hardware experiments with the modulo ADC demonstrate the robustness of our method in a realistic, noisy and low-sampling rate settings, thus validating its high practical utility in a variety of applications.

Index Terms— ADC, modulo, non-linear reconstruction, sampling, sparse recovery, super-resolution.

1. INTRODUCTION

Practical implementation of the Shannon–Nyquist sampling framework entails pointwise acquisition of a continuous-time signal via an analog-to-digital converter (ADC). Such samples are prone to signal clipping or saturation and this poses a fundamental bottleneck when it comes to digital sensing. In a series of companion papers [1–7], the Unlimited Sensing Framework (USF) was introduced as an alternative to Shannon-Nyquist sampling paradigm. The goal of the USF is to acquire signals which are way beyond the dynamic range of a conventional ADC, thus overcoming the dynamic range barrier that is fundamental to conventional sampling framework.

The USF enables High Dynamic Range (HDR) capture by basing itself on a *joint-design* of hardware and algorithms. This is different from the Shannon–Nyquist methodology where hardware and reconstruction algorithms are decoupled from each other. More precisely, before capturing pointwise samples, in the USF, a modulo

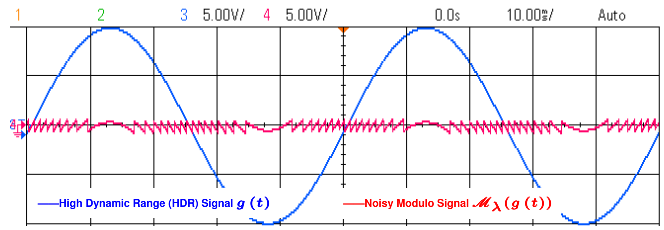

Fig. 1. Oscilloscope screenshot of a sine-wave at the output of our modulo ADC or $\mathscr{M}_\lambda$–`ADC` [5].

non-linearity of the form,

$$\mathscr{M}_\lambda : g \mapsto 2\lambda \left(\left[\!\left[\frac{g}{2\lambda} + \frac{1}{2} \right]\!\right] - \frac{1}{2} \right), \quad [\![g]\!] \stackrel{\text{def}}{=} g - \lfloor g \rfloor, \quad \lambda \in \mathbb{R}^+ \tag{1}$$

where $\lfloor g \rfloor = \sup \{ k \in \mathbb{Z} | \, k \leqslant g \}$ (floor function) is injected in the sampling pipeline. By design, an arbitrary HDR continuous-time signal is folded back into the ADC's dynamic range $[-\lambda, \lambda]$, thus preventing saturation or clipping; a hardware example is shown in Fig. 1. Thereon, the *folded signal* is sampled in a pointwise fashion. This constitutes the modulo ADC or $\mathscr{M}_\lambda$–`ADC` architecture,

$$\text{Input } g(t) \rightarrow \boxed{\mathscr{M}_\lambda(\cdot)} \rightarrow \boxed{\text{Sampling}} \rightarrow y[n] = \mathscr{M}_\lambda(g(nT)).$$

Once the folded samples are acquired, we use novel, mathematically guaranteed, recovery algorithms that amount to "inverting" the $\mathscr{M}_\lambda(\cdot)$ operator; this enables recovery of HDR signal from its low dynamic range, modulo samples.

A hardware prototype for $\mathscr{M}_\lambda$–`ADC` was introduced in [5]. It was experimentally demonstrated in [5] that signals in the span of up to 30λ can be recovered in practice. Subsequently, beyond algorithmic efforts, the effectiveness of USF via initial hardware experiments was explored in a variety of contexts.

Motivation. Our work is motivated by the issues that arise at the intersection of theory and practice of the USF. Currently, there are two algorithms that have been validated on the $\mathscr{M}_\lambda$–`ADC` hardware.

1. The first method is the unlimited sampling algorithm or `US-Alg` introduced in [1] which was initially designed for noiseless scenarios. This method works for signals on the real line. It was adapted for the case of bounded noise in [2] but requires substantial oversampling (see Theorem 3, [2]). A different time-domain algorithm was developed in [7] that can handle measurement non-idealities by working with a generalized version of modulo non-linearity. Similar to the `US-Alg`, the approach in [7] also requires oversampling.
2. The second method is the "Fourier-Prony" algorithm or `FP-Alg`. This method operates in the Fourier domain; it was designed for

The work of the authors is supported by the UK Research and Innovation council's FLF Program "Sensing Beyond Barriers" (MRC Fellowship award no. MR/S034897/1). Further details on Unlimited Sensing and upcoming materials on *reproducible research* are available via `https://bit.ly/USF-Link`.

signals on a finite interval (*e.g.* periodic signals), offers the tightest possible sampling rate (see Theorem 2, [5]), and is agnostic to λ. Through extensive experiments, [5,6,8], the `FP-Alg` is known to be robust to system noise and perturbations that arise in practice. Recently, a modified version of `FP-Alg` was proposed in [9]; this method uses an alternative spectral fitting method in the `FP-Alg` together with time-domain constraints and requires λ to be known.

For real-world applications, one may only measure signals on a finite interval. In this case, the `US-Alg` is not applicable. While `FP-Alg` offers a competitive performance, it suffers from a bottleneck that is intrinsic to the *Fast Fourier Transform* (FFT) implementation, that is, *spectral leakage*. Whenever the modulo samples suffer from spectral leakage, `FP-Alg`-like methods *e.g.* [9] perform sub-optimally and may completely fail depending on the severity of spectral leakage. This necessitates the development of a robust, low-sampling-rate, FFT-free algorithm that can handle signals on finite intervals and offer a competitive performance on $\mathscr{M}_\lambda$–`ADC` hardware.

Contributions. In this paper, we present the **Iter**ative **Si**gnal **S**ieving algorithm or `IterSIS-Alg` that overcomes the limitations of `US-Alg` and `FP-Alg`. The key features of `IterSIS-Alg` are as follows.

1. **Agnostic to Spectral Leakage.** A finite observation window implies leakage in the Fourier domain; this creates algorithmic challenges for extracting the bandlimited. Since `IterSIS-Alg` operates in the time-domain, this is no longer a bottleneck.
2. **Robustness.** The combination of quantization and system noise can lead to non-ideal measurements. This is particularly a problem for the estimation of instants where modulo folds occur. The `IterSIS-Alg` is empirically robust to both bounded and unbounded noise models.
3. **Tight Sampling Rates.** Signal recovery from a small amount of data samples is preferable in practice as a large oversampling rate puts forward higher demand on sampling hardware. The phase-transition curve in Fig. 4 shows that in noisy scenarios, `IterSIS-Alg` operates with moderate oversampling.

2. SAMPLING PIPELINE AND PROBLEM FORMULATION

In this paper, we will focus on arbitrary Ω–bandlimited, square-integrable functions, $g \in \mathcal{B}_\Omega$ observed within a finite time window of size t_0 to match the practical scenarios. Previously, we assumed periodic boundary conditions in [5] to avoid spectral leakage when applying FFT but this is not the case in this paper. Uniform sampling of $g(t), t \in [0, t_0)$ with sampling step $T > 0$ gives rise to samples $\{g[n] = g(nT)\}_{n=0}^{N-1}$, where $N = \lfloor t_0/T \rfloor$. In our context, the modulo samples are contaminated by quantization and system noise (*e.g.* additive Gaussian), denoted by $e[n]$, and are expressed as

$$y_e[n] = \underbrace{\mathscr{M}_\lambda(g(nT))}_{y[n]} + e[n]. \quad (2)$$

This signal model mimics the hardware experiments implemented with the $\mathscr{M}_\lambda$–`ADC`, which accurately describes the practice (see later experiments in Sec. 5).

Goal. Given N *noisy* modulo measurements $\{y_e[n]\}_{n=0}^{N-1}$, our goal is to recover the unfolded samples $g[n]$; thereafter $g \in \mathcal{B}_\Omega$ is recovered via Shannon interpolation as soon as the samples $g[n]$ are known.

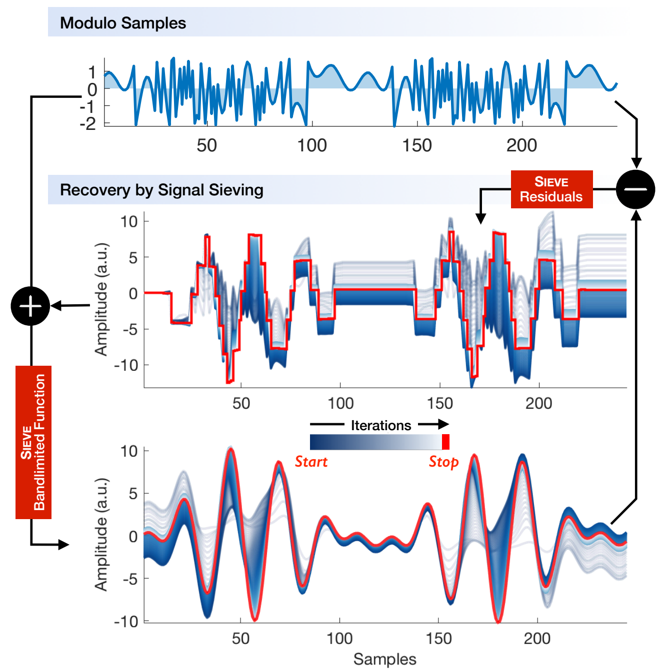

Fig. 2. Flowchart of the iterative signal sieving (`IterSIS-Alg`).

3. ROBUST RECOVERY METHOD

Overview of Recovery Method. We begin our discussion with the modular decomposition property [2] that leads to the representation,

$$g = \mathscr{M}_\lambda(g) + \varepsilon_g, \quad t \in [0, t_0), \quad \varepsilon_g(t) = \sum\nolimits_{k=0}^{K-1} c_k \mathbb{1}_{\mathcal{D}_k}(t) \quad (3)$$

where $c_k \in 2\lambda\mathbb{Z}$, $\varepsilon_g(t)$ is the residue function and $\mathbb{1}_\mathcal{D}$ is the indicator function on domain D with $\cup_m \mathcal{D}_k = \mathbb{R}$. The key to our recovery approach is a *sieving approach*; the modulo samples are decomposed into two sieves satisfying the respective constraints for g and ε_g,

$$\underbrace{\mathscr{M}_\lambda(g)}_{\text{Modulo Signal}} \stackrel{(3)}{=} \underbrace{g \in \mathcal{B}_\Omega}_{\text{Bandlimited Sieve}} + \underbrace{\varepsilon_g \in 2\lambda\mathbb{Z}}_{\text{Residual Sieve}}. \quad (4)$$

The notion of "sieving" is similar to the idea of how separating signals based on their structure. To give the reader an idea about the `IterSIS-Alg` (see Algorithm 1), we show the action of our method on hardware data (Experiment 4 in [5]) in Fig. 2. The algorithm iterates (blue curves) till a stopping criterion is met and the reconstruction is achieved (red curve).

Instead of operating on (4), we operate in the finite-difference or Δ domain,

$$\Delta y[n] = \Delta g[n] - \sum\nolimits_{k=0}^{K-1} c_k \delta[n - n_k] \equiv (\Delta g - \Delta \varepsilon_g)[n] \quad (5)$$

where $\{c_k, n_k\}_{k=0}^{K-1}$ encode the unknown folding instants due to the $\mathscr{M}_\lambda$–`ADC`. Obviously, the number of folding instants depends on the setup of the $\mathscr{M}_\lambda$–`ADC` threshold λ. When working with noisy modulo samples (2), we have, $\Delta y_e[n] = \Delta y[n] + \Delta e[n]$ where $e[n]$ arises from quantization and system noise. This data corruption together with a finite observation window yields spectral leakage out of the bandwidth. Hence, the previous strategies of high-order difference [1,2] or Fourier domain partitioning [5,6,8] may not apply.

In our work, we will directly operate in the time-domain by sieving the signal according to (5).

Sieve #1: Spike Estimation. We utilize a continuous-time characterization of $\Delta\varepsilon_g[n] = \sum_{k=0}^{K-1} c_k \delta[n-n_k]$ as $g[n]$ can be easily obtained by removing the residue $\Delta\varepsilon_g[n]$ from $\Delta y[n]$ and applying the anti-difference operator. Given a Dirac mass $\delta[n-n_0], n_0 \in \mathbb{Z}, n \in [0, N-1]$, we leverage the following parameterization[1],

$$\delta[n-n_0] = \frac{1}{N}\frac{\sin\big((n-n_0)\pi\big)}{\sin\left((n-n_0)\pi/N\right)} \equiv \frac{1}{N}\frac{1-e^{\jmath 2\pi(n-n_0)}}{1-e^{\jmath 2\pi(n-n_0)/N}}. \quad (6)$$

In other words, (6) provides a continuous model to characterize the spike. Given a stream of K shifted spikes, (6) translates to,

$$\Delta\varepsilon_g[n] \overset{(5),(6)}{=} \sum_{k=0}^{K-1} \frac{\breve{c}_k}{1-e^{-\jmath\frac{2\pi n_k}{N}} e^{\jmath\frac{2\pi n}{N}}} = \frac{\mathsf{P}_{K-1}\left(\xi_N^n\right)}{\mathsf{Q}_K\left(\xi_N^n\right)} \quad (7)$$

where,

- $\mathsf{P}_{K-1}\left(\xi_N^n\right)$ and $\mathsf{Q}_K\left(\xi_N^n\right)$ are polynomials of degree $K-1$ and K, respectively with $\xi_N^n = e^{\jmath\frac{2\pi n}{N}}$.
- $\breve{c}_k = \left(1-e^{-\jmath 2\pi n_0}\right)c_k/N$.

In fact, $\mathsf{Q}_K\left(\xi_N^n\right)$ corresponds to an annihilation filter (*i.e.* Prony's method); its roots uniquely encode the spike-locations n_k in $\Delta\varepsilon_g[n] = \sum_{k=0}^{K-1} c_k\delta[n-n_k]$. Note that, ratio in (7) has $2K$ degrees of freedom; this is exactly the number of unknown parameters $\{c_k, n_k\}_{k=0}^{K-1}$ in $\Delta\varepsilon_g$. Hence, $\Delta\varepsilon_g$, can be exactly recovered once these polynomial coefficients of $\mathsf{P}_{K-1}\left(\xi_N^n\right), \mathsf{Q}_K\left(\xi_N^n\right)$ are known.

Sieve #2: Bandlimited Projection. We do not require exact bandlimitedness, rather desire energy concentration in the low-pass region. We do so by implementing circular convolution,

$$g_\Omega[n] = (g * \psi_\Omega)[n] \quad \text{(Bandlimited Projection)} \quad (8)$$

where $\psi_\Omega[n] \in \mathcal{B}_\Omega$ is an ideal low-pass filter. Also since, $g_\Omega \in \mathcal{B}_\Omega \Rightarrow \Delta g_\Omega \in \mathcal{B}_\Omega$, we apply (8) to Δg to ensure bandlimitedness.

Stopping Criterion. Perturbations make it challenging to propose a general noise model for $e[n]$ in (2). This motivates us to move our attention from noise statistics to deterministic uncertainty in the data. Hence, we base our *stopping criterion* on a deterministic noise margin—the "MSE budget" (cf. [10, 11]).

Iterative Signal Sieving Method. Combining the above ingredients, the modulo signal recovery can be formulated as the following quadratic minimization problem

$$\min_{\substack{\mathsf{P}_{K-1},\mathsf{Q}_K\\ \Delta g_\Omega}} \sum_{n=0}^{N-1}\left|\Delta y[n] - \Delta g_\Omega[n] - \frac{\mathsf{P}_{K-1}\left(\xi_N^n\right)}{\mathsf{Q}_K\left(\xi_N^n\right)}\right|^2 \quad (9)$$

for which we opt to use a linear minimization strategy that leads to a fast and efficient solution. In particular, we solve for,

$$\min_{\substack{\mathsf{P}_{K-1}^{[i]},\mathsf{Q}_K^{[i]}\\ \Delta g_\Omega}} \sum_{n=0}^{N-1}\left|\frac{\Delta\left(g_\Omega - y\right)[n]\,\mathsf{Q}_K^{[i]}\left(\xi_N^n\right) - \mathsf{P}_{K-1}^{[i]}\left(\xi_N^n\right)}{\mathsf{Q}_K^{[i-1]}\left(\xi_N^n\right)}\right|^2. \quad (10)$$

Solving the above quadratic minimization problem for $\mathsf{Q}_K^{[i]}$ provides a collection of candidates for $\mathsf{Q}_K\left(\xi_N^n\right)$, when $i = 1 \ldots i_{\max}$, out of which we choose the one for which the MSE is the smallest. Note that, our goal is not to minimize the MSE for (9), rather we aspire to find a valid solution that fits our noisy modulo data up to an uncertainty characterized by the "RMSE budget" or $\mathsf{RMSE} = \sqrt{\frac{1}{N}\sum_{n=0}^{N-1}|e[n]|^2}$. In other words, we consider the modulo signal recovery to be successful as soon as the fitting error in (9) is no larger than the RMSE budget. Next, in Sec. 4, we develop an efficient implementation of this principle that follows an alternative strategy.

[1] Of course, many other models (*e.g.* polynomials) can also be used in our context. However, applying a parsimony principle, the Dirichlet kernel in (6) is more robust and flexible, in terms of model sparsity and complexity.

Algorithm 1 Iterative Signal Sieving for Modulo Sampling

Input: Modulo Samples $y[n]$ and Bandwidth Ω

Estimate: $K = \{\mathrm{card}(\mathcal{I}) \,|\, |\Delta y[i]| \geqslant \lambda, i \in \mathcal{I}\}$.
Initialize $\Delta\widetilde{\varepsilon}_g^{[0]}[n] = \Delta y[n]$.

for $i = 1$ to $i_{\max}$ **do**

Update the spike estimate $\Delta\widetilde{\varepsilon}_g^{[i]}[n] \leftarrow \Delta\widetilde{\varepsilon}_g^{[i-1]}[n]$ by fitting $\Delta\widetilde{\varepsilon}_g^{[i-1]}[n]$ with the polynomial fraction model in (11).

Obtain the BL estimate $\Delta\widetilde{g}_\Omega^{[i-1]}[n] = \Delta y[n] + \Delta\widetilde{\varepsilon}_g^{[i]}[n]$.

Update the BL signal estimate $\Delta\widetilde{g}_\Omega^{[i]}[n] \leftarrow \Delta\widetilde{g}_\Omega^{[i-1]}[n]$ by performing low-pass filtering (8).

Check the MSE stopping criterion: if satisfied, stop the iteration; otherwise, keep iterating.

end for

Obtain the $\widetilde{g}_\Omega[n]$ by applying the anti-difference operator Δ^{-1}.

Output: The recovered BL signal $\widetilde{g}_\Omega[n]$.

---

4. ITERATIVE SIGNAL SIEVING ALGORITHM

To implement the *signal sieving principle*, we solve the quadratic minimization problem in (10). More specifically, the minimization (10) can be decomposed as two sub-optimization problems as illustrated below.

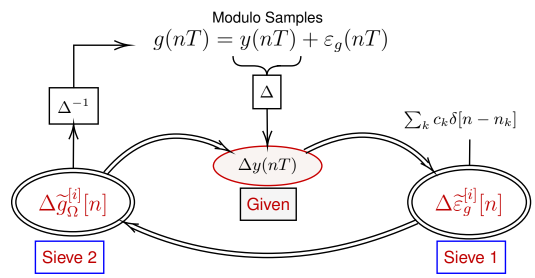

Sub-problem: Spike Estimation. Update the estimate $\Delta\widetilde{\varepsilon}_g^{[i-1]} = (\Delta\widetilde{g}_\Omega^{[i-1]} - \Delta y)$ by performing model-fitting on $\Delta\widetilde{\varepsilon}_g^{[i-1]}[n]$. Denoting by $\mathbf{V}_N^M$ the $N \times M$ inverse DFT matrix: $\mathbf{V}_N^M = \frac{1}{N}\left[\xi_N^{nm}\right]_{n,m}$, where $n \in [0, N-2]$,$m \in [0, M-2]$, the polynomials involved in (9) can be expressed algebraically as $\left[\mathsf{P}_{K-1}\left(\xi_N^n\right)\right]_n = \mathbf{V}_N^K\mathbf{p}$ and $\left[\mathsf{Q}_K\left(\xi_N^n\right)\right]_n = \mathbf{V}_N^{K+1}\mathbf{q}$, respectively, where $\mathbf{p}$ and $\mathbf{q}$ are the coefficients of $\mathsf{P}_{K-1}\left(\xi_N^n\right)$ and $\mathsf{Q}_K\left(\xi_N^n\right)$. Let $\mathbf{R}^{[i-1]}$ be the inverse $N \times N$ diagonal matrix with elements $\mathrm{diag}\left(\mathbf{V}_N^{K+1}\mathbf{q}^{[i-1]}\right)^{-1}$. Then, given an spike estimate $\Delta\widetilde{\varepsilon}_g^{[i]}[n]$, at iteration i, the sub minimization can be reformulated as

$$\{\mathbf{p}^i, \mathbf{q}^i\} = \arg\min_{\mathbf{p},\mathbf{q}} \left\|\mathbf{A}^{[i-1]}\mathbf{q} - \mathbf{B}^{[i-1]}\mathbf{p}\right\|^2 \quad (11)$$

where $\mathbf{A}^{[i-1]} = \mathrm{diag}\big(\Delta\widetilde{\varepsilon}_g^{[i]}\big)\mathbf{R}^{[i-1]}\mathbf{V}_N^{K+1}$ and $\mathbf{B}^{[i-1]} = \mathbf{R}^{[i-1]}\mathbf{V}_N^K$. In order to ensure a unique solution $\mathbf{q}^i$ to (11), we impose $(\mathbf{q}^0)^{\mathsf{H}}\mathbf{q}^i =$

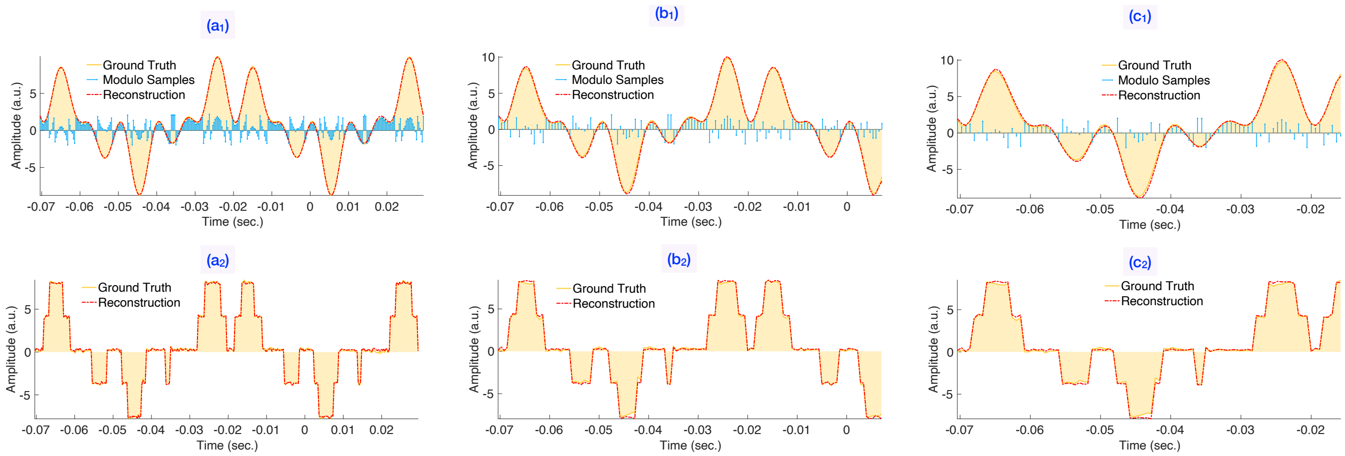

Fig. 3. Hardware experiments. (a) Recovery with noisy modulo samples (15% noise, $N = 334$ samples with $K = 32$ folding instants). (b) Recovery with a small sampling rate ($N = 130$ samples with $K = 26$ folding instants). (c) Recovery with spectral leakage: (c) is a truncated version of (b) ($N = 92$ samples with $K = 21$ folding instants). This signal truncation yields significant spectral leakage which leads to the failure of Fourier-domain partitioning algorithms. However, the proposed approach achieves an accurate reconstruction despite noise contamination and spectral leakage. For (a)-(c), the signal dynamic range is $\max |g(nT)| = 9.53\lambda$.

1 with initialization $\mathbf{q}^0$. The number of spikes can be robustly estimated by evaluating the significant jump of the finite difference of the modulo samples: $K = \{\text{card}(\mathcal{I}) | |\Delta y[i]| \geqslant \lambda, i \in \mathcal{I}\}$.

Sub-problem: Bandlimited Projection. From the update $\Delta\widetilde{\varepsilon}_g^{[i]}[n]$, we obtain and update the bandlimited signal estimate,

$$\left(\Delta\widetilde{\varepsilon}_\Omega^{[i-1]} + \Delta y\right) \mapsto \Delta\widetilde{g}_\Omega^{[i-1]} \longrightarrow \boxed{\psi_\Omega} \xrightarrow{(8)} \Delta\widetilde{g}_\Omega^{[i]} = \Delta\widetilde{g}_\Omega^{[i-1]} * \psi_\Omega.$$

Stopping Criterion. We compute the reconstructed RMSE using $\Delta\widetilde{\varepsilon}_g^{[i]}[n], \Delta\widetilde{g}_\Omega^{[i]}$. Once it is smaller than or equal to the predefined RMSE budget, the iterations stop; otherwise, go to Step 1 and keep iterating[2]. Fig. 2 describes the visual output of the signal sieving process. An algorithmic implementation is provided in Algorithm. 1.

5. EXPERIMENTAL VALIDATION

In the noiseless scenario, the signal recovery is exact. In order to reveal the interplay between all possible ingredients, *e.g.* number of samples or spikes, RMSE budget, etc., we conduct the following simulation. We keep the number of spikes fixed ($K = 20$) and observe the reconstructed RMSE versus different number of samples and RMSE budget, as shown in Fig. 4. Clearly, with a small amount of samples, our algorithm achieves an accurate signal recovery that fits the modulo data within the RMSE budget. Larger the RMSE budget (*i.e.* stronger the noise), higher is the number of samples needed.

Then, we move to the hardware experiments based on the US-ADC to validate the performance of the proposed algorithm. A continuous signal is generated by a `TTi TG5011` waveform generator. Its output is then split into 2 channels fed to the `DSO-X 3024A` oscilloscope with inbuilt ADC, yielding the modulo samples $y[n]$ and the conventional samples (our ground truth). The ADC threshold $\lambda = 2.01$ and the specific experimental settings are given in the table,

[2]This RMSE can be obtained by pre-calibration, or from the instrument parameters. If the RMSE budget is unknown, we simply run the algorithm of a fixed number of iterations and choose the reconstruction that yields the minimum RMSE. We refer the interested readers to [10] for more details.

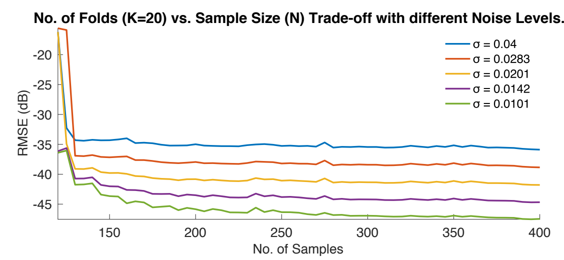

Fig. 4. Sampling Evaluation: Recovery with different number of samples and RMSE budget. The number of folding instants is fixed $K = 20$ and the dynamic range $\max |g(nT)|$ is 7λ.

	T (ms)	Run time (s)	$\lceil \frac{\Omega}{2\pi} N \rceil$	RMSE Budget	N	K	Recovered RMSE
Fig. 3 (a)	0.30	1.79	25	0.1279	334	32	0.0930
Fig. 3 (b)	0.60	1.04	27	0.1883	130	26	0.1869
Fig. 3 (c)	0.30	0.92	20	0.2344	92	21	0.2052

Using Step 1) of Algorithm. 1, the number of spikes is accurately estimated which is consistent with the sparsity of $\Delta(g_\Omega[n] - y[n])$. The signal reconstructions of $g_\Omega[n], \varepsilon_g[n]$ are presented in Fig.3, for which the resulting RMSEs are all below the budgets. The dynamic range $\max |g(nT)|$ in Fig.3 (a)-(c) is 9.53λ. In all cases, the proposed algorithm achieves robust and accurate recovery, which demonstrates its performance in a realistic setting. We do not compare our method to `FP-Alg`-like methods [5, 9] as they use FFT-domain processing which fails in the presence of spectral leakage.

6. CONCLUSION

In this paper, we presented a novel algorithm "ITER-SIS" for modulo signal recovery. Hardware experiments have shown that ITER-SIS is robust to noise and achieves reconstruction with low-sampling-rate. Since ITER-SIS is FFT-free, it is particularly of interest where spectral leakage is an issue. Proving convergence and recovery guarantees for ITER-SIS remain interesting future research directions.

7. REFERENCES

[1] A. Bhandari, F. Krahmer, and R. Raskar, "On unlimited sampling," in *Intl. Conf. on Sampling Theory and Applications (SampTA)*, Jul. 2017. [Online]. Available: https://doi.org/10.1109/sampta.2017.8024471

[2] ——, "On unlimited sampling and reconstruction," *IEEE Trans. Signal Process.*, vol. 69, pp. 3827–3839, Dec. 2020.

[3] ——, "Methods and apparatus for modulo sampling and recovery," US Patent US10 651 865B2, May, 2020.

[4] A. Bhandari and F. Krahmer, "HDR imaging from quantization noise," in *IEEE Intl. Conf. on Image Processing (ICIP)*, Oct. 2020, pp. 101–105.

[5] A. Bhandari, F. Krahmer, and T. Poskitt, "Unlimited sampling from theory to practice: Fourier-Prony recovery and prototype ADC," *IEEE Trans. Signal Process.*, vol. 70, pp. 1131–1141, Sep. 2021.

[6] A. Bhandari, "Back in the US-SR: Unlimited sampling and sparse super-resolution with its hardware validation," *IEEE Signal Process. Lett.*, vol. 29, pp. 1047–1051, Mar. 2022.

[7] D. Florescu, F. Krahmer, and A. Bhandari, "The surprising benefits of hysteresis in unlimited sampling: Theory, algorithms and experiments," *IEEE Trans. Signal Process.*, vol. 70, pp. 616–630, Jan. 2022.

[8] A. Bhandari, "Unlimited sampling with sparse outliers: Experiments with impulsive and jump or reset noise," in *IEEE Intl. Conf. on Acoustics, Speech and Signal Processing (ICASSP)*, May 2022, pp. 5403–5407.

[9] E. Azar, S. Mulleti, and Y. C. Eldar, "Residual recovery algorithm for modulo sampling," in *IEEE Intl. Conf. on Acoustics, Speech and Signal Processing (ICASSP)*, May 2022.

[10] R. Guo, Y. Li, T. Blu, and H. Zhao, "Vector-FRI recovery of multi-sensor measurements," *IEEE Trans. Signal Process.*, vol. 70, pp. 4369–4380, Sep. 2022.

[11] R. Guo and T. Blu, "FRI sensing: Retrieving the trajectory of a mobile sensor from its temporal samples," *IEEE Trans. Signal Process.*, vol. 68, pp. 5533–5545, Sep. 2020.